NASA Contractor Report 165801

NASA-CR-165801
19820012688

Design and Fabrication of Brazed René 41 Honeycomb Sandwich Structural Panels for Advanced Space Transportation Systems

Andrew K. Hepler and Allan R. Swegle

Boeing Aerospace Company
Kent, Washington 98031

CONTRACT NAS1-14213
DECEMBER 1981

National Aeronautics and
Space Administration

Langley Research Center
Hampton, Virginia 23665

NASA Contractor Report 165801

Design and Fabrication of Brazed René 41 Honeycomb Sandwich Structural Panels for Advanced Space Transportation Systems

Andrew K. Hepler and Allan R. Swegle

Boeing Aerospace Company
Kent, Washington 98031

CONTRACT NAS1-14213
DECEMBER 1981

National Aeronautics and
Space Administration

Langley Research Center
Hampton, Virginia 23665

This Page Intentionally Left Blank

FOREWORD

This program was performed by Boeing Aerospace Company; Kent, Washington for the National Aeronautics and Space Administration, Langley Research Center (NASA LaRC) under NASA Contract 1-14213 from March, 1978 through August, 1980. Mr. John L. Shideler, of the Thermal Structures Branch, Structures and Dynamics Division, LaRC, was Technical Monitor for the program.

Boeing Program Manager was Mr. Allan R. Swegle under the administration of Mr. Andrew K. Hepler. Contributors to the program are as follows:

G. A. Dishman	Design
A. R. Swegle	Stress
V. Deriugin	Thermal Analysis

This Page Intentionally Left Blank

TABLE OF CONTENTS

LIST OF FIGURES

LIST OF FIGURES

SUMMARY

The objective of this program was to design and fabricate large brazed Rene'41 honeycomb panels, to establish a test plan to subject the panels to cyclic thermal gradients and mechanical loads equivalent to those imposed on an advanced space transportation vehicle during its boost and entry trajectories, and to design and fabricate a test fixture for the cyclic tests.

Two Rene'41 brazed honeycomb panels were designed and fabricated. The panels were sized to be subjected to combined cyclic thermal and mechanical loads and combined thermal and ultimate mechanical laods. The panels will be tested to measure and evaluate stresses induced by thermal gradients and mechanical loads. Test conditions include both high thermal and high mechanical loads typical of integral cryogenic tank hot structures space vehicle boost conditions and moderate thermal and low mechanical loads of typical high temperature entry conditions. Analysis data and discussion of the design conditions are included in this report. The analysis data will be compared later to the test data.

AMI 937 used in Phase I and II of this contract is the selected braze alloy. The panels are 30.48 cm (12 inches) by 182.88 cm (72 inches) by 3.05 cm (1.2 inches) deep. The panels were designed to be supported at four locations providing three spans, two outer spans of 45.72 cm (18 inches) and one inner span of 76.2 cm (30 inches). The middle span provides a representation of thermal and mechanical stress levels and distributions found in the continuous spans in a typical multiframe/spar bay hot structures entry space vehicle. The two panels are sized to give different stress levels in the interior support areas.

INTRODUCTION

The objective of this program was to design and fabricate large brazed Rene'41 honeycomb panels and establish a test plan to subject the panels to cyclic thermal gradients and mechanical loads equivalent to those imposed on an advanced space transportation vehicle, Ref. 1, during its boost and entry trajectories. Further, the test fixtures were to be fabricated.

Various programs of advanced space transportation systems have included hot structures designs, with (Ref. 2) and without metal-heat shields (Refs. 1 and 3). The Reference 1 and 3 studies used the body and wing of the entry vehicle to house the fuel and oxidizer to feed the propulsion system required for orbital insertion. The conditions imposed on the panels built under this program match those for a low wing loading entry vehicle with liquid hydrogen and liquid oxygen integral tanks and no external heat shields. The data would also be applicable to a lesser extent to higher wing loading entry vehicles with some form of thermal protection system.

The subsequent future test program will record the separate and integrated strains induced by thermal gradients and mechanical loads. A vehicle life time of boost and entry cycles will be imposed on the panels. At the end of the cyclic program, the panels will be mechanically loaded to failure at peak boost thermal conditions.

PANEL DESIGN

Panel elements were selected to be representative of the surface panels on an advanced space transportation vehicle (Ref. 1) with low wing loading during entry from orbit. The external surface requires no additional thermal

protection and the inside surfaces form the containers for liquid hydrogen fuel or liquid oxygen. The Ref. 1 vehicle has a design life of 500 cycles.

A three span test configuration was chosen to simulate the multiple spans of surface panels over frames and spars on the lower surface of an advanced entry vehicle. The middle span of 76.2 cm (30 in.) matches the frame and spar spacing of the Ref. 1 vehicle. The outside span lengths are chosen to permit development of a load distribution that results in panel stresses representative of those experienced on a flight vehicle. The overall shears and moments and skin stress levels in the middle span are comparable to those in the continuous spans of the entry vehicle.

The sizing and mechanical loading of the two specimens were designed to provide a higher stress level in Specimen 2 than that in Specimen 1. The same thermal input is imposed on both specimens, but Specimen 1 has chem-milled pads to locally reduce the stress levels imposed by thermal and mechanical loads.

The stress levels for Specimen 1 were selected to follow design criteria established for the Reference 1 vehicle (i.e. stress levels equal to or less than the proportional limit) and are based on the following limit and ultimate stress levels. Design limit tension stress for Rene'41 structure is selected to be 689 MPa (100 ksi) at 88K (-300^{o}F) and design limit compression stress is selected to be 607 MPa (88 ksi) at 455 K (360^{o}F). Design ultimate compression stress is selected to be 758 MPa (110 ksi) and .0058 strain at ultimate load at 455 K (360^{o}F). The proportional limit is taken to be 869 MPa (126 ksi) in tension at 77 K (-320^{o}F) and 613 MPa (88.9 ksi) in compression at 455 K (360^{o}F). Typical longitudinal core shear failure stress

determined from limited test data for the 150.6 kg/m^3 (9.4 lb/ft^3) core used in both panels is 3.37 MPa (490 psi) at room temperature.

The Specimen 2 skin compression stress levels are increased above the Specimen 1 levels to evaluate the effect of sustaining operating stresses above the proportional limit but less than 0.2 percent offset yield stress. Imposing stresses above the proportional limit on Specimen 2 at the inner supports will allow an assessment of the effect of the thermal environment imposing strains rather than stresses on the specimen and what this effect may have on cyclic loading.

Figure 1 illustrates the stress and strain effects of combined mechanical and thermal loads application at the inner supports during the course of ultimate load testing after cyclic tests. Above the compression yield stress an elastic combination of mechanical and thermal stresses in the spanwise direction may be computed which will be somewhat greater than the actual combined stress level, Figure 1. The combined actual compression strain level will significantly exceed the addition of mechanically and thermally induced compression elastic strain levels at the supports. The plastic strain generated will contribute to a reduction of the overall thermal strain imposed on the specimen. This thermal strain reduction will be manifested as a significant stress change in elastically stressed areas away from the supports on the test specimen and a small reduction of stress at the support where the specimen is stressed into the plastic range as shown in Figure 1. At the center of the test specimen inner span where thermal stress subtracts from the mechanical stress, less thermal stress will be subtracted from the mechanical stress as plastic strains increase at the supports.

In the hot structure vehicle design, it is important to determine how close normal operating stress levels may approach, or in the case of short lived vehicles, the extent they may exceed the proportional limit without developing excessive deformation on successive cycles. Specimen 2 will be subjected to stress level of 83 MPa (12 ksi) above proportional limit while Specimen 1 will be subjected to a stress level of 55 MPa (8 ksi) below the proportional limit.

It is also important to determine ultimate load and stress level after imposing a life time of operating stress levels. Ultimate design criteria for a hot structure design will likely include compression design criteria for pressurized structure such as: "The stress at 2.0 times the operating pressure stress plus 1.25 times the thermal stress should not exceed the allowable compression stress". This type of criteria may be adequate at the supports where thermal stresses add to the pressure stresses. The ultimate design criteria may have to be modified for panel structure between the points of counterflexure on the inner span where thermal stresses reduced by plasticity at the supports subtract from pressure stresses.

Significant weight savings in hot structures designed for low cyclic life can be achieved by exposing the compression structure to operating stresses near the proportional limit. Ultimate skin design criteria may be less critical than the operating criteria in a ductile material such as Rene'41 if full advantage is taken of strain design and strain allowables in considering internal loads imposed by the thermal environment.

Panel details are shown in Figures 2 and 3. In Figure 2, Specimen 1 is distinguished from Specimen 2 by its two .0635 cm (.025 in.) thick by 19.05 cm (7.5 in.) wide chem-milled pads in the hot side or outer skin. The basic skin gage of both panels is .053 cm (.021 in.) gage. The .127-.229 cm (.05-.09 in.) wide slot in the hot side skin in the longitudinal center of each specimen shown in Figure 3 provides relief from thermal stresses/strains.

Specimen 2 has additional 15.24 cm (6 in.) long slots located mid-way between the edge and the continuous center slot. These two short slots are located so that they are bisected by the test fixture interior supports centerlines. The short slots are so placed to evaluate the effect of additional relief of transverse core shear and core axial stresses caused by constraint of thermally induced deformations at panel support points. Slot effects on panel skin and core stresses are discussed in the section entitled "Panel Design Analysis".

PANEL DESIGN LOAD CONDITIONS

Mechanical loads plus thermal conditions will be imposed on the panels so that stresses in inner and outer skins at the interior support locations will simulate stress levels that would be experienced during a spaceflight vehicle operation.

Mechanical loads will be applied equally by a load distribution system at four locations on the panel. Load locations and support points are shown in Figure 4. The three span configuration and the magnitude and locations of the test mechanical loads were chosen to simulate structural arrangement and the internal pressures generated by LH_2 fuel containment of the Reference 1 vehicle. The magnitudes of the mechanical loads required to obtain the desired stresses are given in the section "Panel Design Analysis".

The input temperatures were determined by the boost and entry thermal conditions sustained by the Reference 1 vehicle. Although entry temperatures influence material selection, boost conditions are critical to sizing on the Reference 1 vehicle. Boost conditions have higher differential temperatures between inner and outer skins which will generate higher thermal stresses than occur during entry. Fuel tank pressures are higher during boost than during entry. The fuel is exhausted from the tank at the end of the boost period. A comparison of boost

and entry conditions is shown in Figure 5. Figure 5 also presents a comparison of thermally induced lower surface skin stresses during boost and entry, assuming equal inner and outer skin gages. The vehicle design temperatures were modified for the panel tests so that appropriate thermal differences will occur even though liquid nitrogen (LN_2) at 77.3 K (-320^{o}F) will be substituted for the vehicle's LH_2 fuel at 20 K (-423^{o}F). The temperatures were also modified to account for increases in thermal strains in the center span which are calculated to be approximately 14% greater than that calculated for a continuous panel which spans many supports uniformily spaced at 76.2 cm (30 in.).

Consequently, test thermal stresses and strains will be induced by simulated boost conditions with a peak 455.2 K (360^{o}F) hotside temperature and a 88.4 K (-300^{o}F) cold side temperature and by simulated entry temperatures on the hotside to a maximum 1033.6 K (1400^{o}F). The panel test temperature profiles for boost and entry conditions are shown in Figures 6 and 7 respectively. Mechanical loads will be combined with these thermal loads during the tests. In Figure 6, it is specified that the outer skin should be cooled to the temperature range of 166 K (-160^{o}F) to 255 K (0^{o}F) following the attainment of the peak temperature and prior to initiating heating for the next cycle. This broad range is specified in order to minimize test costs and time rather than to wait for the entire outer skin to come to a uniform equilibrium temperature. It means that absolute minimum stresses in the cycle could be up to 103 MPa (15 ksi) higher than if outer skin equilibrium temperatures were attained before a subsequent cycle was initiated. The more time efficient conduct of the test is considered more important than the small increase in the minimum cyclic thermal stress.

PANEL DESIGN ANALYSIS

Separate and combined loads and stresses for the panels are shown in Figures 8 through 16. Boost environment shear and moment diagrams are shown for Specimen 1 in Figure 8. Thermal shears and moments for Specimen 2 will be virtually the same as for Specimen 1. Specimen 2 has a mechanical load input of 7006 N (1575 lb.) per point and its shear and moment diagrams developed for mechanical loads will be proportionately increased over those of Specimen 1 which has a 4359 N (980 lb.) per point input.

A finite element analysis was conducted on Specimen 2 by Mr. James Robinson of NASA Langley Research Center. The computer analysis was run prior to the addition of the two 15.24 cm (6 in.) long slots which were centered on the interior support locations (See Figure 3). The accuracy of the analysis remains unchanged on the side of the panel which has six inch slot spacing with no intermediate slots. Hot side boost peak temperature of 472 K (390^{o}F) was incorporated in the analysis which was later modified to 455 K (360^{o}F) for the test. The computer model is shown in Figure 17.

The computer analysis fixed the vertical displacement of the nodes across the width of the specimen on the hot side at the supports. In the test fixture, the test specimen will be forced against rigidized fiberfrax (silica fibers) pads, approximately 0.254 cm (0.10 in.) thick, which separate the panel from the supports on the hot side as shown in Figure 4. The pads serve as insulators to prevent heat loss from the hot skin to the cold support. The pads will not restrain lateral expansion of the skins due to temperature change but will support the panel by bearing reaction only, and their lower spring rate will tend to permit the panel to compress the pads, allowing the panel to assume a more freely deformed shape under test thermal and mechanical load environments than is assumed in the computer analysis.

In the Ref. 1 vehicle, the surface panel is restrained by the integrally attached frame at the cold inner skin, whereas the test panel is reacted in bearing on the hot outer skin against the padded test fixture. Skin stresses for the model are similar in magnitude and variation to those for the Ref. 1 vehicle. However, core normal stresses at the vehicle frame are opposite in sign to those at the model support because of the way the loads are applied and reacted. The Ref. 1 vehicle fuel pressure imposes a net tension force on the core at the frame as contrasted by the test reactions causing a net compression force in the core. Additional comparisons of vehicle, model and test panel loads, reactions and stresses follow in later sections.

Face Sheet Stresses

A finite element analysis was conducted on a model simulating the six-inch slot spacing and sizing of Specimen 2. The finite element model was constrained as shown in Figure 17 in the Z direction on all nodes on its width at X = 0 and X = 45.72 cm (18 in.). This constraint affects panel behavior in a similar manner as a stiff frame. The constraint, like a very stiff frame, provides resistance to the panel bowing in the Y direction caused by the thermal gradients imposed on the panel. This constraint causes a sharp peaking of X-direction thermal skin stresses midway between the six-inch slots at the supports as shown in Figure 9. The influence of constraint at the supports on the mechanically applied load induced skin stresses is relatively minor as shown in Figure 9 and as evidenced by the more uniform level of stresses across the width of the specimen at the support.

The results of hand analyses of the panels shown in Figures 10 and 11 for Specimens 1 and 2 respectively, assume support at the frame but do not assume that the panel is constrained from bowing in the Y direction at the supports. An effort was made to estimate the peaking of stresses at the supports caused by

vertical constraint across the width based on the Specimen 2 finite element analysis, as indicated by the dashed lines in Figures 10 and 11. The hand analysis assumes that the panels will behave as a beam rather than a wide panel because of the six-inch slot spacing. General agreement of the hand analysis and the finite element analysis away from the frame proves this assumption. The purpose of the six-inch slot spacing is to reduce core shear stresses, to reduce Y-direction skin thermal stresses to negligible values, and to reduce X-direction skin thermal stresses approximately 30% by reducing the Poisson ratio influence found in wide plates. The intermediate six inch long slots over the supports (see Figure 3) have virtually no additional effect on X-direction skin stresses but further reduce core shear stresses. The influence of slots on core shear stress is discussed in the section entitled "Core Stresses".

Specimen 1 as shown in Figure 10 is sized and loaded to provide at the interior supports a skin compression stress of approximately -572 MPa (-83 ksi) and a tension stress of 689 MPa (100 ksi) if full constraint is available at the support. If the panel bowing due to thermal distortion in the Y-direction is not constrained, the skin compression stress will be -482 MPa (-70 ksi) and the skin tension stress will be 607 MPa (88 ksi). The influence of the skin pad on outer skin stress levels over the support is shown in Figure 10.

Specimen 2 is sized and loaded to provide an elastic skin compression stress of -807 MPa (-117 ksi) as shown in Figure 11 if full constraint is available or -710 MPa (-103 ksi) if full panel thermal distortion in the Y-direction occurs. The elastic tension skin stresses for Specimen 2 will be 807 MPa (117 ksi) as shown in Figure 11 if constrained and 117 MPa (103 ksi) if not constrained. As mentioned previously, the compression operating stress level of the Specimen 2 outer skin is above the proportional limit of approximately -613 MPA (-88.9 ksi), see Figure 1. This will result in a small amount of local plasticity at the support on the

compression skin which will cause a small amount of thermal strain relief. The unconstrained stress levels shown in Figure 11 are more likely to be achieved because the panel is supported in bearing against the support. There may be a small reduction in peak stresses due to some redistribution of stress across the width of the specimen and a small amount of thermal strain relief caused by operating in the plastic range.

The hand analysis which assumes no constraint of panel thermal distortion in the Y-direction and the computer analysis which provides full Z-direction constraint at the support establish the bounds or limits of the maximum skin stress levels that will occur over the supports during the test. As indicated previously, the test panels will be forced against the rigidized fiberfrax bearing and insulation pads on the test fixture supports by the reaction forces of the mechanically applied loads and the thermal environment. It is anticipated that the mechanical forces may affect the bowing in the Y-direction at the support which is discussed in more detail in the section "Core Stresses". It is recognized that the Z-direction constraint of the finite element model more closely reflects the direct attachment to a frame immersed in LH_2 fuel of the reference vehicle. The test skin stresses can be modified to equal the stress levels indicated by the finite element model at the supports by increasing the mechanically applied loads as necessary.

Ultimate panel mechanical loads with the boost thermal environment imposed on Specimens 1 and 2 are shown in Figure 12. Face skin compression failure stresses over the support were assumed to be at the compression yield stress of 758 MPa (110 ksi) and .0058 strain at 455.2 K ($360^{o}F$). The .053 cm (.021 in.) gage of Specimen 2 may cause failure at a slightly lower stress than the stress on the .064 cm (.025 in.) gage of Specimen 1. The .064 cm (.025 in.) gage skin

on Specimen 1 will be capable of sustaining significantly more strain than the .053 cm (.021 in.) gage skin on Specimen 2 at the interior supports because Specimen 1 has a small intracell buckling stability advantage over Specimen 2. For example, if a given skin gage and core combination fails at F_{C_Y}, as shown in Figure 1, a small gain in stress failure level by changing skin gage may result in a large increase in allowable strain level. These facts may alter the mechanically induced failure loads - raising the load on Specimen 1 relative to the load on Specimen 2. The possibility of not achieving the mechanical load levels shown in Figure 12 because of core failure is discussed in section "Core Stresses".

CORE STRESSES

A hand core shear analysis was conducted on the honeycomb core of Specimens 1 and 2. The results are tabulated in Figure 13. The assumptions involved in the analysis include uniform and unconstrained support of the panel at the support points shown in Figure 4 and uniform distribution of core shear stress through the depth and across the width (Y-direction) of the specimens. The analysis shows zero core shear stress in the inside span core due to thermal loading because no external shear load is applied by thermal loading between interior support points. The analysis shows a decrease in thermally induced longitudinal core shear stress from limit load to ultimate load in the outside span. This phenomena is caused by the reduction of skin stress and thermally induced internal load when the combination of mechanical and thermally induced loads increase the skin stress level above the proportional limit stress. This subject is also discussed in the sections entitled "Face Skin Stress" and "Panel Design" and is shown in Figures 1, 9 and 11. The reduction of thermally induced skin stress and load at ultimate load also results in a reduction of

thermally induced moment and a consequent reduction of the equal and opposite sign shear reactions at outer and inner support points shown in the limit shear plot in Figure 8. The core shear stress in the outer span is directly proportional to the outer support point shear reaction load. The hand analysis results, for mechanical loads, as shown in Figure 13, indicate that the inside span of each specimen has more highly loaded core than the outside spans but that the core shear stress on either specimen does not exceed the core shear strength of 3.37 MPa (490 psi) of the honeycomb core.

The finite element model used to analyze Specimen 2 included only the slot on the panel longitudinal (X-direction) centerline outer skin. The core shear stress results of the computer analysis data are shown in Figures 14 and 15 for the thermally induced and mechanical loads respectively. The core shear results reflect the influence of the Z-direction constraint at the supports. The Z-constraint closely matches the behavior of panel attachment to a frame held at the same temperature as the inner skin. As shown in Figure 14, the thermally induced longitudinal core shear stress (XZ plane) on the inner span averages zero as in the hand analysis but varies from 4.8 MPa (696 psi) near a slot to -2.74 MPa (-397 psi) midway between slots. Similar results are shown for the outer span. The thermally induced transverse core shear stress varies from -3.6 MPa (-522 psi) near a slot to 3.6 MPa (522 psi) at the next adjacent slot and zero midway between slots. The transverse stress and the wide positive and negative variation of longitudinal stress is caused by the combination of Z-direction restraint and the expansion of the hot outer skin between the slots (in the Y-direction) and the contraction of the cold inner skin in the Y-direction. Figure 16 displays the mechanical and thermal load caused core normal stress at an interior support point. These stresses include the reaction load compression stresses (represented by the average stresses) as well as the tension and compression stresses

generated by the Z-direction constraint which prevents out of plane thermally induced displacement at the interior support. The peak thermally induced longitudinal and transverse core shear stresses fall off rapidly with increasing X-direction distance from the support. The affects of the constraint on the mechanically induced core shear stresses displayed in Figure 15 show less deviation from the hand analysis than the thermally induced core shear stresses.

The hand analysis and the finite element analysis bracket the possible core shear and core axial load stresses that can be generated in the test specimens. The finite element model results indicate that a total of 26.9 kN (6040 lb.) tension loads are adjacent to the slot and edges required to constrain the thermally induced out of plane displacement of Specimen 2 at the interior support. The interior support reaction load due to the limit mechanical loads of Specimen 1 and Specimen 2 are 8 kN (1800 lb.) and 12.9 (2890 lb.) respectively. The mechanical loads imposed during the test will tend to flatten the displacement caused by thermal distortion. If this flattening is proportional to the reaction loads caused by the mechanical loads divided by the thermally induced reaction tension loads indicated by the finite element model, then Specimen 1 may be influenced to approximately 30% and Specimen 2 to 48% of the level of full constraint at the interior supports at limit loads. These percentages are probably reduced to a certain extent by the spring rate of the rigidized fiberfrax support insulation pads.

The 150.6 kg/m^3 (9.4 lb/ft^3) honeycomb core available for this program has an ultimate core shear stress of approximately 3.38 MPa (490 psi) at room temperature. The ultimate core crushing stress is estimated to be at least 5.86 MPa (850 psi). If the panels when subjected to higher mechanically applied loads during ultimate load tests approach the constraint at the supports which was used in the finite element model, then the ultimate mechanical loads shown in

Figure 12 (based on face skin failure) may be reduced by approximately 42% (ultimate core crushing stress divided by normal core stress at support, see Figure 16). Near full Z-direction constraint, the panels will be critical in core shear or core crushing or a combination of core shear and core crushing rather than being skin critical.

The method in which the test panels react the mechanically and thermally induced loads in the area of constraint relative to the method in which panels of the Ref. 1 vehicle react mechanically and thermally induced loads in the area of a vehicle frame have been discussed. Other factors of difference between the Reference 1 vehicle and the test configuration include the following. In the typical interior frame of a series of regularly space frames in the Ref. 1 vehicle there is no significant net reaction load to thermally induced panel moments. The positive and negative longitudinal core shear stresses similar to those shown in Figure 14 must balance to zero average core shear stress. The thermally induced core axial stresses at the frame must balance to zero between the slots and are in compression near the slots and in tension midway between the slots.

PANEL FABRICATION

Materials and processes specifications for the panels are noted in Figure 2. The panels utilize 150 kg/m^3 (9.4 lb/cu. ft.) Rene'41 honeycomb core throughout each panel in order to not incur the cost of splicing lighter cores in the low shear zones.

AMI 937 (developed as 930 FOB) braze alloy was used. A braze alloy weight of 1860 gm/m^2 (1.2 gm/sq. in.) on the top surface (hot side) and 1550 gm/m^2 (1.0 gm/sq. in.) on the lower surface were selected in order to reduce developmental costs in refining the braze weight to the least amount required for

.48 cm (3/16 in.) cell size core. Previous development would indicate that at least a 20% reduction from this braze weight on this cell size core could be anticipated.

Braze temperature was 1353 K (1975^{o}F). Following brazing, the panel temperature was dropped to 1200 K (1700^{o}F) and held for one hour and then cooled to room temperature. Typical room temperature tensile properties following brazing and also following subsequent exposure to 500 simulated entry cycles to a maximum of 1006 K (1350^{o}F) are shown in Figure 18. The tensile data, taken from Reference 4, shows that additional aging has occurred during cyclic exposure to the entry cycles.

Figure 19 shows sheet measurements on the as-received upper face sheet of Specimen 1 prior to chem-milling. Figure 20 shows the same sheet thicknesses after chem-milling.

A cold spot developed during the brazing of both panels in virtually the same location and size area. A furnace element was found to be missing in the furnace base. The graphite base fixture plates conducted sufficient heat to affected areas to just initiate flow. The areas were located in the outer spans where they will be subjected to low face skin and core stresses. A pattern of bolts was placed in the affected areas as shown in Figure 21 and 22. The affected zone was determined by examination of X-rays.

A strip of tooling core used around the edges of the test panels, extended into the structural area of Specimen 2. The tooling core was fabricated from rejected Rene'41 foil which was supplied by an alternate rolling mill. This foil exhibited varying hues of surface oxidation. This variable surface oxide caused inconsistent results in acceptance test braze operations. The tooling core was used because of the limited quantity of acceptable Rene'41 honeycomb

core available for this contract. A 1.02 cm (0.4) inch strip was cut from Specimen 2 as shown in Figure 22 along its long edge to eliminate the tooling core thereby reducing panel width from 30.48 cm (12 in.) to 29.46 cm (11.6 in.).

TEST FIXTURE DESIGN AND FABRICATION

A test fixture was designed and fabricated to meet ultimate load requirements shown in Figure 12, to provide space for radiant heat lamps to meet the temperature and heating rate requirements of Figures 6 and 7 and to provide the general loading and reaction points configuration of Figure 4.

The test fixture shown in Figure 23 was built about a frame consisting of a 292 cm (115 in.) long beam supported by two vertical columns welded to 2.54 X 61 X 91.4 cm (1 X 24 X 36 inch) base plates. The beam and columns were fabricated from standard A-36 W12 X 65 shapes. The beam height was 135 cm (53 in.) from the floor. The reaction points consisted of welded built up beams supported from the underside of the basic frame beam. The four reaction points interface with the panel as shown in Detail A in Figure 4. The mechanical loads were applied from the underside of the test panel at the four locations shown in Figure 4 by an evener system consisting of three beams on each side of the panel. The evener system was connected on one side to a hydraulic load actuator and on the other side to a reacting load cell. The actuator and load cell were pin connected to cross beams which were in turn, pin connected to a support welded to the top of the frame beam at its center of span.

An open aluminum welded tub 42 X 194 X 71 cm (16.5 X 76.5 X 28 in.) deep was provided to contain the liquid nitrogen (LN_2) used to simulate the Ref. 1 vehicle LH_2 fuel. The NASA Dryden Flight Research Center (DFRC) provided 15.2 cm (6 in.) of poured styrafoam insulation around the closed sides of the

LN_2 tub. The styrofoam was incased in a mating welded aluminum box. The LN_2 container was to be positioned so that the LN_2 level would come to mid-core height of the edge sealed panel. DFRC established that an aluminum tape provided satisfactory edge seals to prevent LN_2 contact against the core.

DFRC designed and provided the radiant heat lamps to impose on the test panels the boost and entry temperatures and heating rates shown in Figures 6 and 7.

CONCLUDING REMARKS

Two Rene'41 brazed H/C panels were designed and fabricated. A test plan was established to subject the panels to cyclic thermal gradients and mechanical loads equivalent to those imposed on an advanced space transportation vehicle during its boost and entry trajectories. A test fixture for the cyclic tests was designed and fabricated. Test conditions include both high thermal and high mechanical loads typical of integral cryogenic tank hot structures space vehicle boost conditions and moderate thermal and low mechanical loads of typical high temperature entry conditions. Analysis data for these conditions are included in this report. The panels, test plan and test fixture were delivered to NASA.

REFERENCES

1. Hepler, A. K., and Bangsund, E. L.: "Technology Requirements for Advanced Earth Orbital Transportation Systems". NASA Contractor Report 2879, Boeing Aerospace Company, 1977.

2. X-20 Dynasoar Program, Air Force Contract AF-33(657)-7132, The Boeing Company, 1963.

3. Taylor, Allan H., and Jackson, L. Robert: "Thermostructural Analysis of Three Structural Concepts for Reusable Space Vehicles". AIAA Paper 79-0874, presented at AIAA/NASA Conference on Advanced Technology for Future Space Systems, Hampton, Virginia, May 8-10, 1979.

4. Lenhart, Herbert G: "Rene'41 Sheet Heat Treat Study" Boeing Aerospace Company, Structural Test Materials Laboratory Tension Lab Data Sheet 2-7800-1 3/69, April 30, 1979.

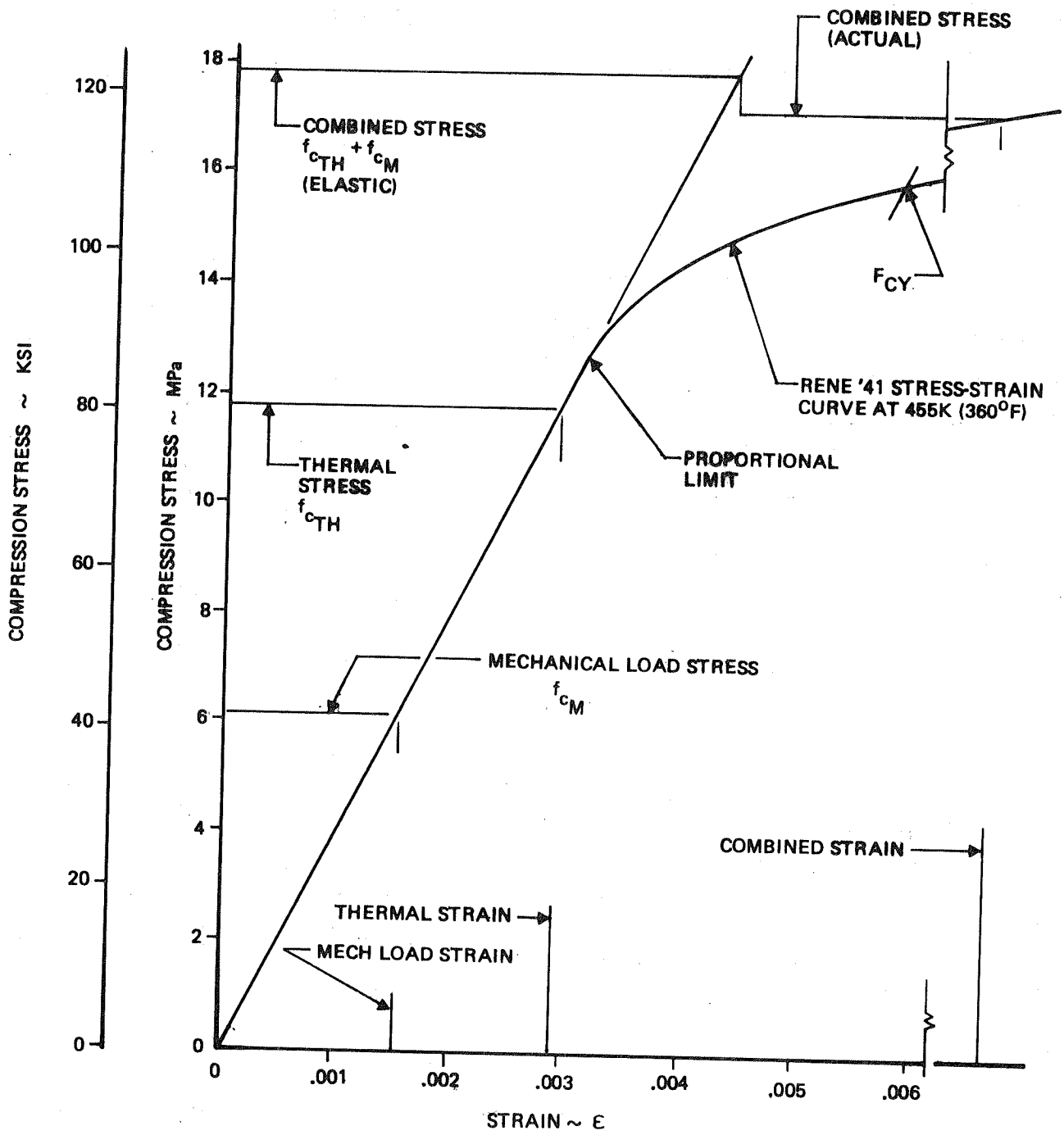

Figure 1. Specimen 2 Compression Stress and Strain of Outer Skin at Interior Supports

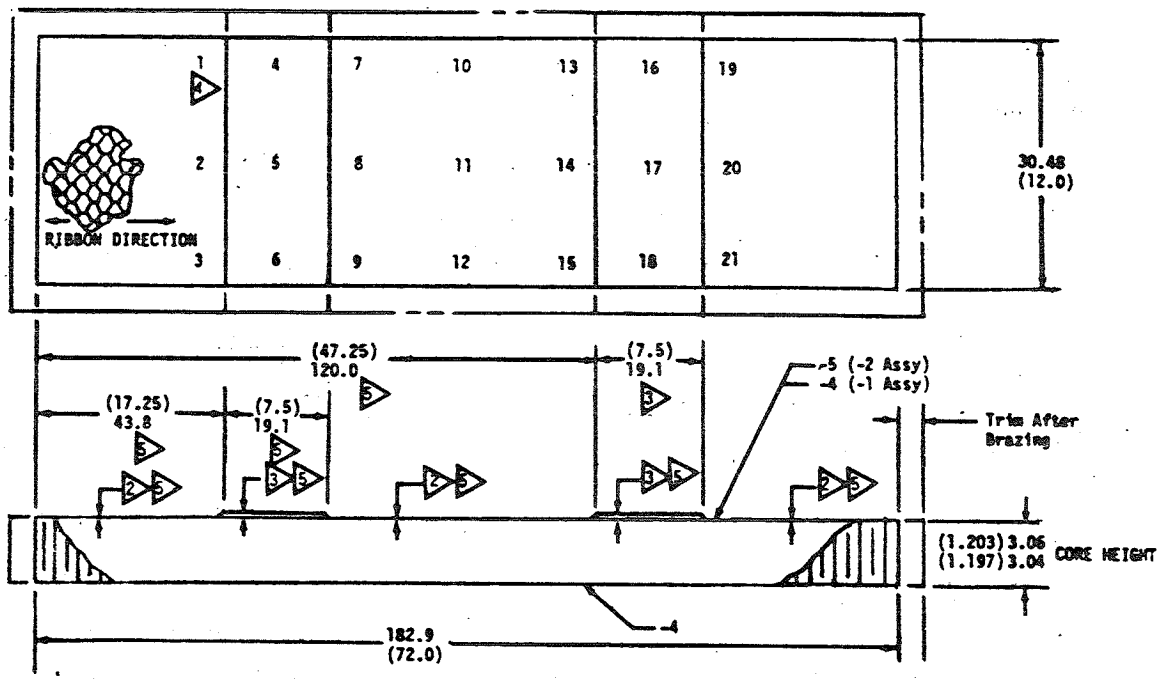

2. .061 (.024) Minimum Skin Thickness
.051 (.020)
Remaining Thicknesses to be as Chem-Milled but not less than .051 (.020) (Only One Place in Entire Panel Need Conform to .061 (.024) DIMN) .051 (.020)

3. .069 (.027) At Minimum Pad Thickness
.064 (.025)
Remaining Thicknesses to be as Chem-Milled - but not less than .064 (.025) (Only One Place in Both Pads Need Conform to .069 (.027) .064 (.025)

4. Record Thickness of -5 Panel After Chem Milling in 21 Locs as shown

5. -5 Skin Only

6. Braze Panel Per Boeing Process Spec - Vacuum Brazing Light Weight Rene'41 Honeycomb Panels

7. Tolerance ± .152 (.06) Unless Otherwise Noted

8. Supplied by Rohr to RMS 110 - Core to be Welded Per Rohr Memo 802-0703 WEL dated Feb 14, 1978 to Boeing Aerospace Company

DIMENSIONS
cm (in.)

QTY REQD	QTY REQD	PART OR IDENTIFYING NO.	NOMENCLATURE OR DESCRIPTION	MATERIAL AND SPECIFICATION
1		-5	Skin .076 (.030) Sht	Rene'41 35.6 X 188 (14 X 74) Per AMS 5545 As Supplied by Boeing
1	2	-4	Skin .053 (.021) Sht	Rene'41 35.6 X 188 (14 X 74) Per AMS 5545 As Supplied By Boeing.
1	1	-3	Core 3.05 (1.2) High	RCB 3-15 Rene'41 Honeycomb Core 35.6 X 188 (14 X 74) 8
-		-2	Panel Assy (Test)	6
	-	-1	Panel Assy (Test)	6

BOEING
PANEL ASSEMBLY TEST ONLY
D 51203 254-20710

Figure 2. Panel Assemblies

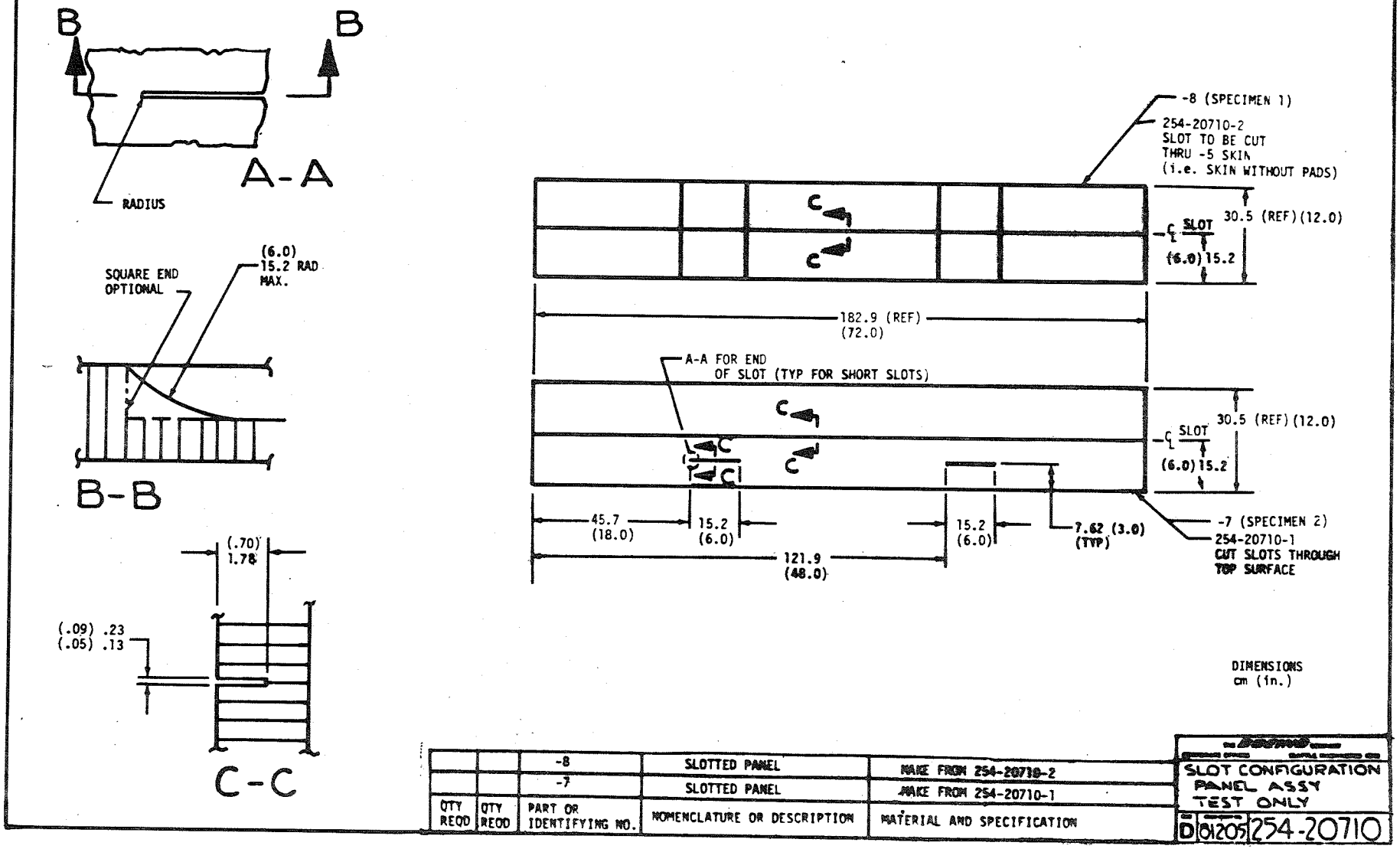

Figure 3. Slot Configurations – Panel Assemblies

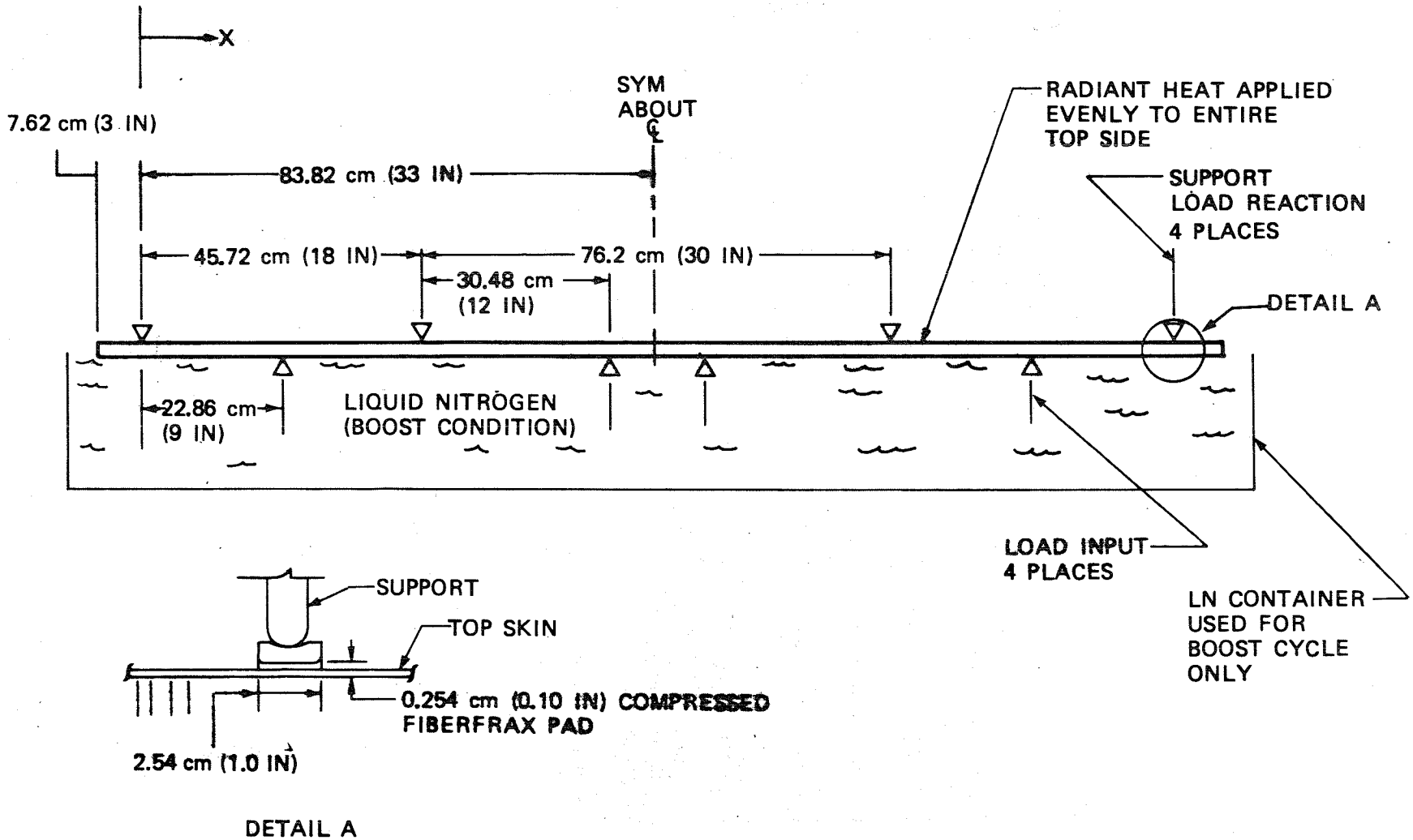

Figure 4. Panel Test Fixture Schematic

	UNITS	BOOST	ENTRY	
			AT MAX. TEMP. RATE	AT MAX. TEMP.
TEMP (INNER SKIN)	K (^{O}F)	20 (-423)	156 (280)	995 (1330)
TEMP (OUTER SKIN)	K (^{O}F)	478 (400)	672 (750)	1034 (1400)
$\frac{1}{2}[E_o(\alpha\Delta T)_o - E_i(\alpha\Delta T)_i]$ (FOR CONDITION COMPARISON ONLY; ASSUMES EQUAL INR & OTR SKIN GA.)	MPa (KSI)	472 (68)	310 (45)	8.3 (1.2)
FUEL TANK PRESSURE	N/m^2 (PSI)	1.16×10^5 (16.8)	1.03×10^4 (1.5)	1.03×10^4 (1.5)

Figure 5. Advanced Space Transportation Vehicle (Ref 1) Boost and Entry Condition Comparison

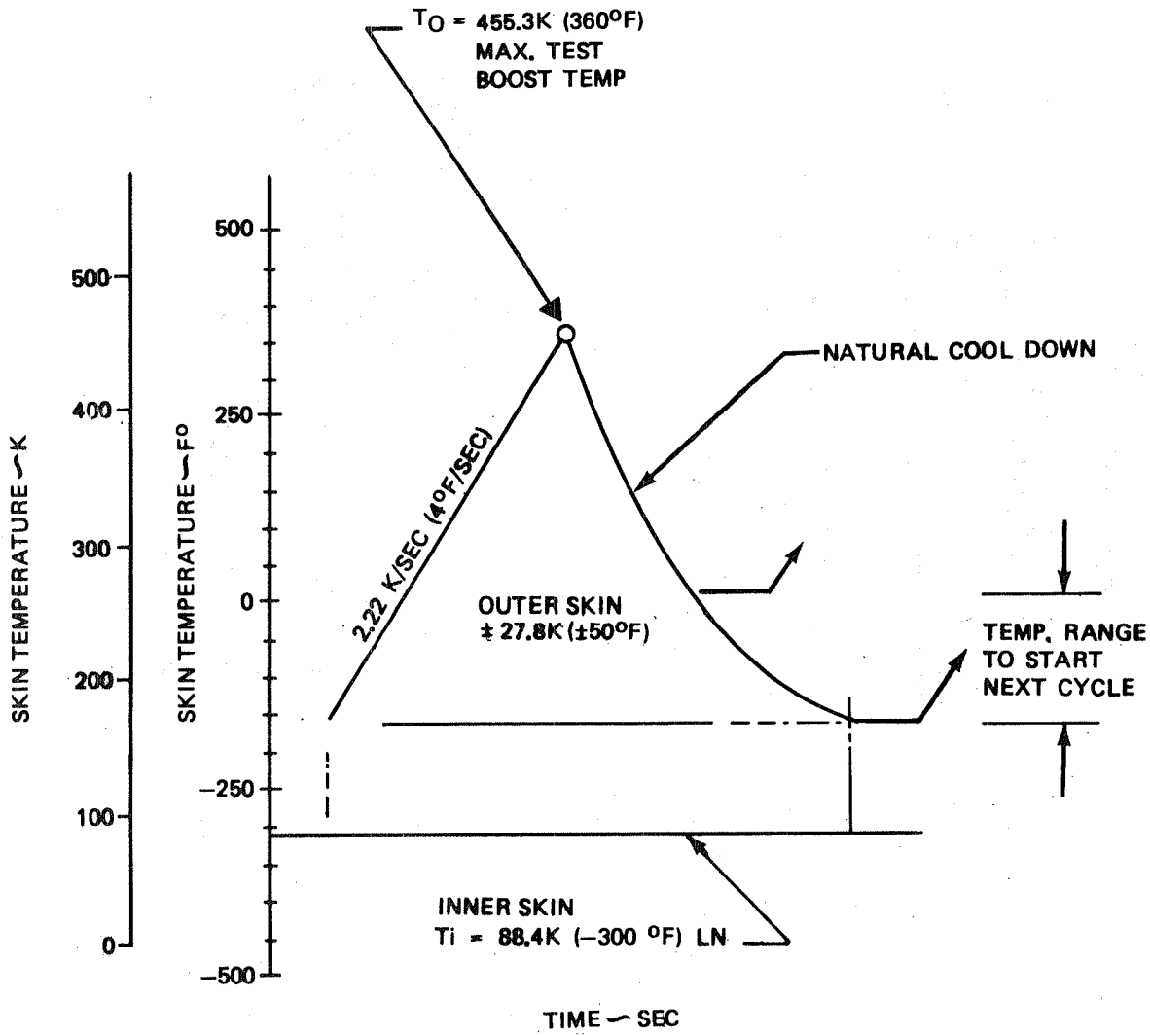

Figure 6. Boost Profile

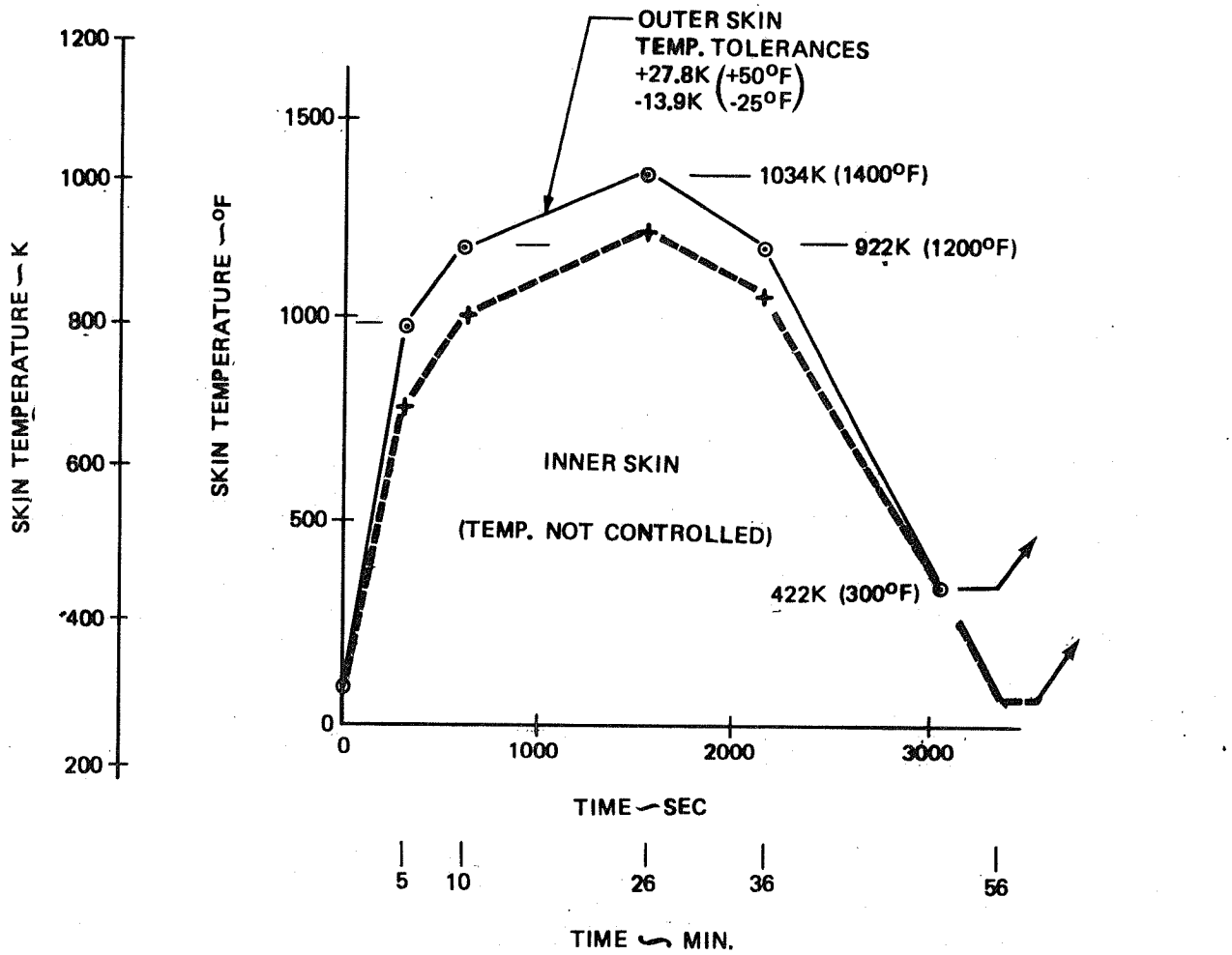

Figure 7. Entry Profile

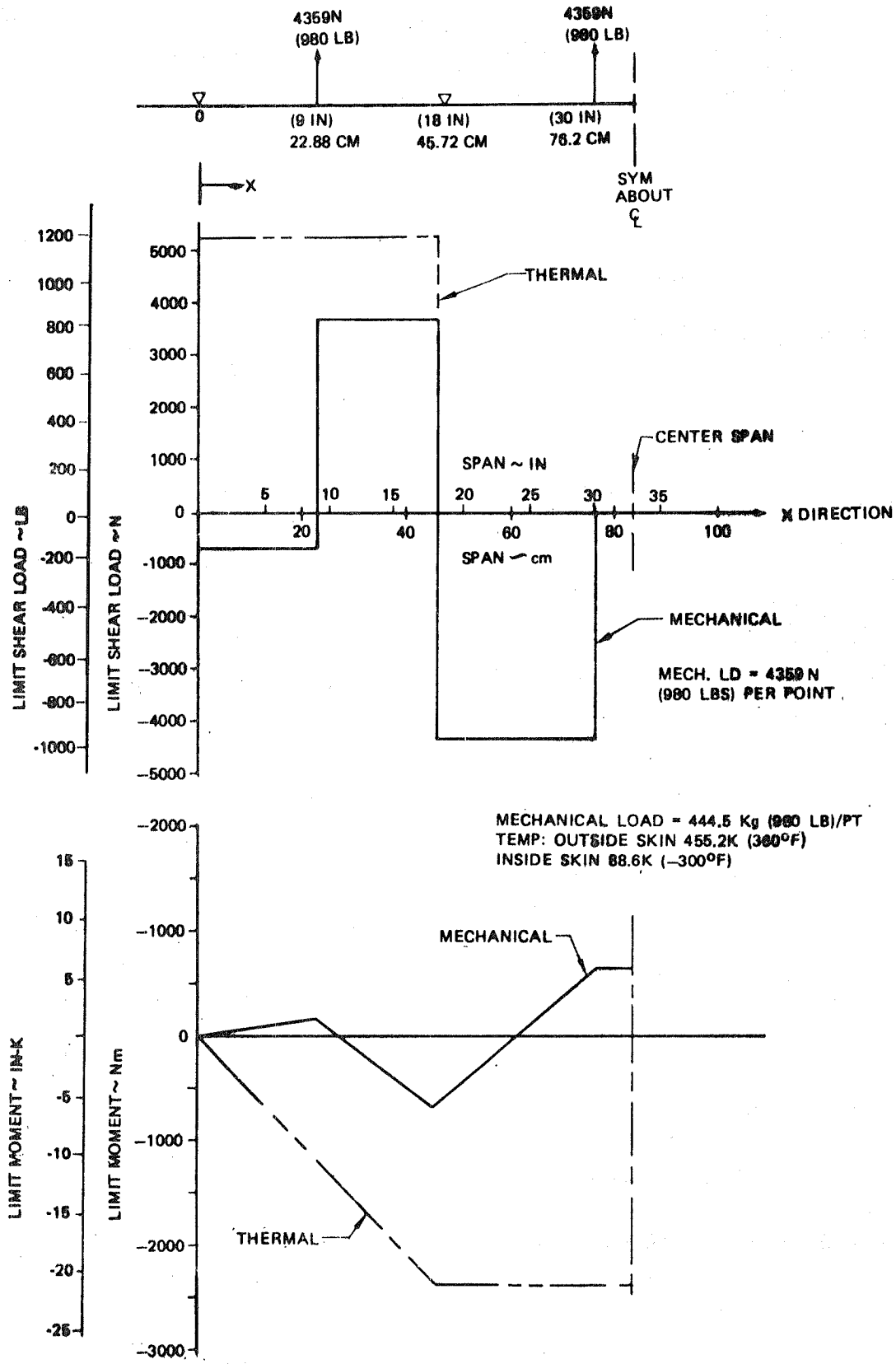

Figure 8. Specimen 1 Limit Shear & Moment Diagrams

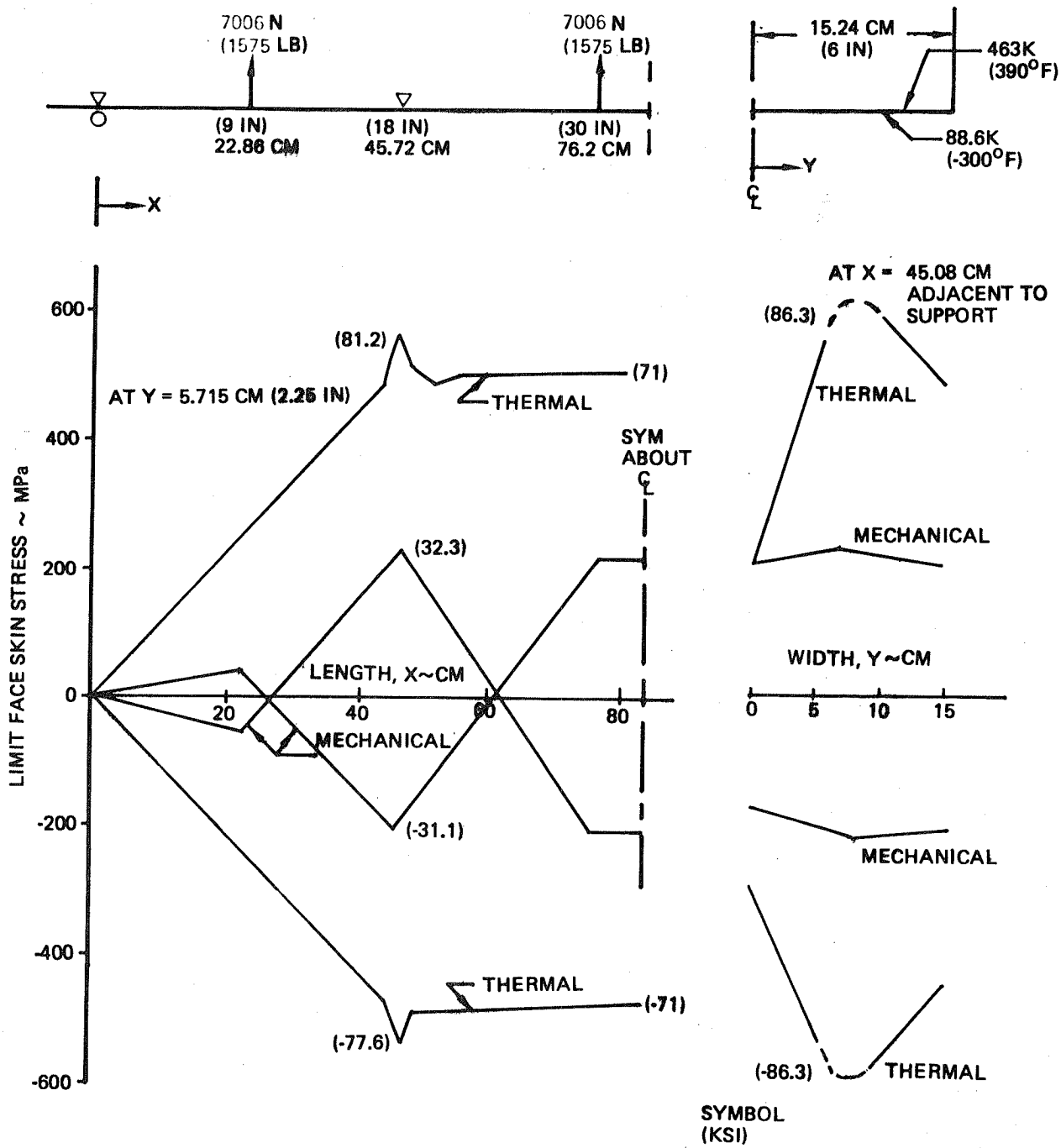

Figure 9. Specimen 2 Limit Face Skin Stresses — Finite Element Analysis

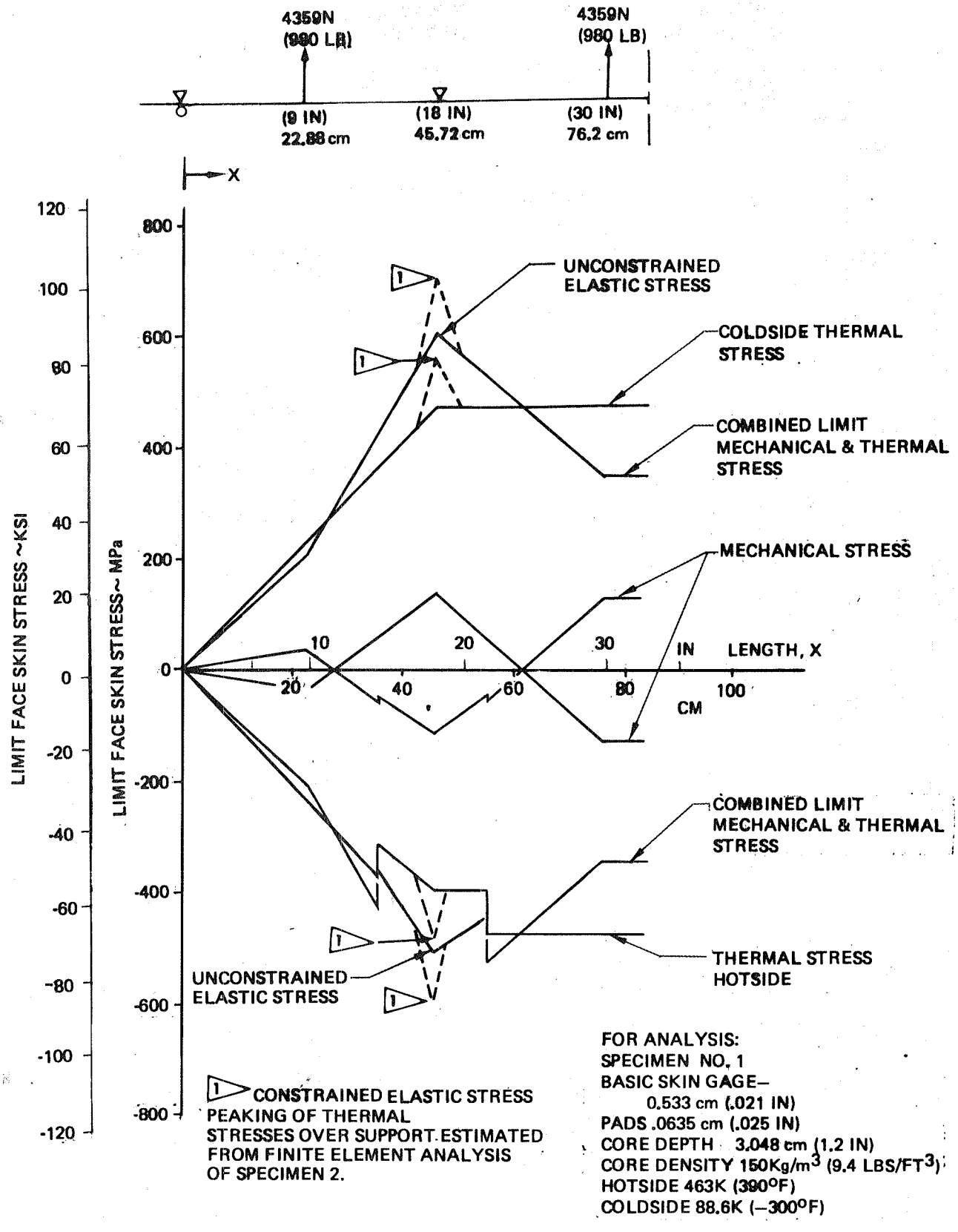

Figure 10. Specimen 1 Limit Face Skin Stresses at Y = 5.715 cm (2.25 in.)

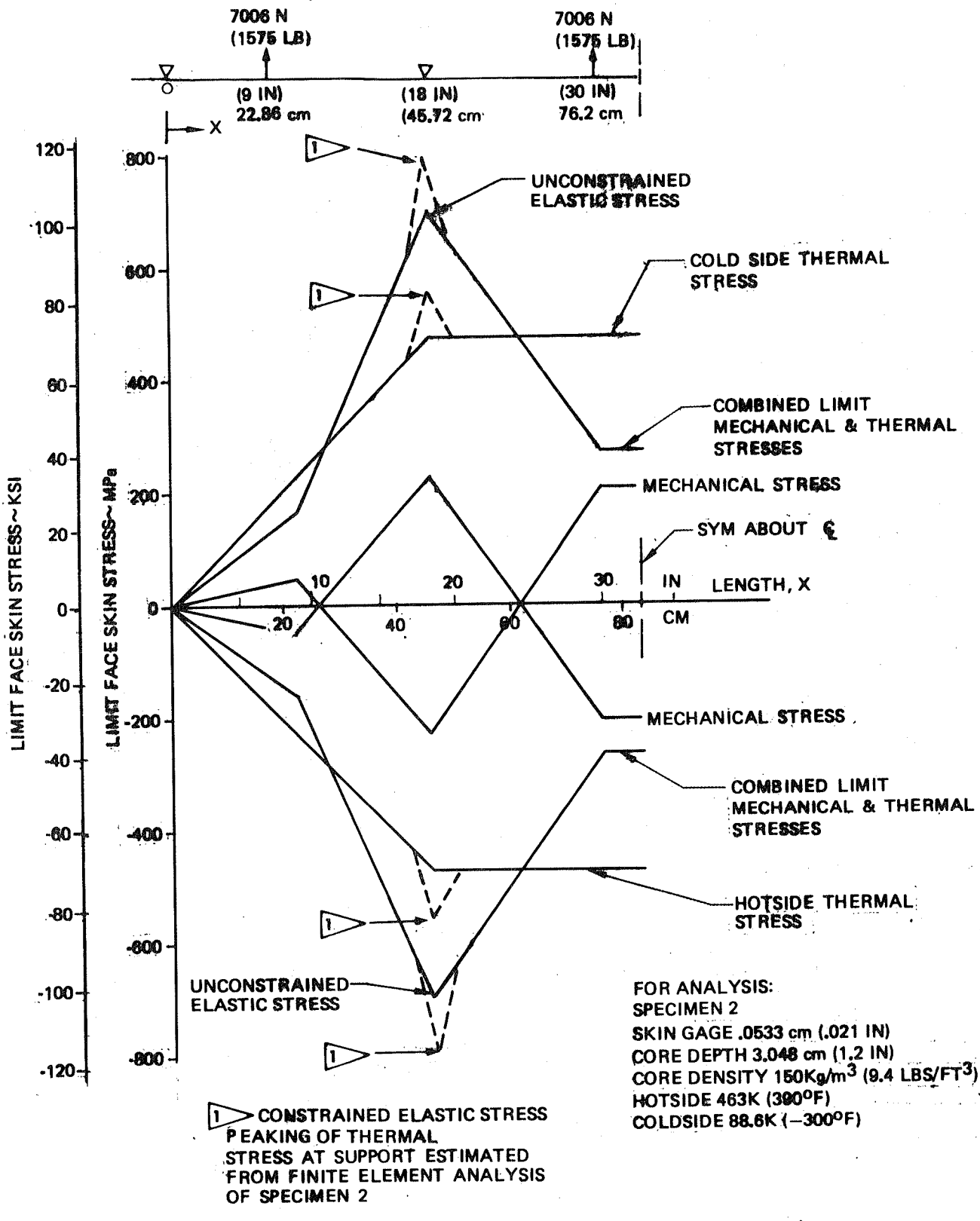

Figure 11. Specimen 2 Limit Face Skin Stresses at Y = 5.715 cm (2.25 IN)

SPECIMEN NUMBER	MECHANICAL FAILURE LOADS PER LOAD POINT [1]		SKIN TEMPERATURE			
			HOT SIDE		COLD SIDE	
	N	LB	K	°F	K	°F
1	28077	6312	455.2	360	88.8	−300
2	23584	5302	455.2	360	88.8	−300

[1] ASSUMES LOCAL FACE SKIN FAILURE AT F_{CY} = 758 MPa (110 ksi) AND .0058 STRAIN ON HOT SIDE AT INTERIOR SUPPORTS

Figure 12. Test Specimens Ultimate Loads

SPECIMEN	INSIDE SPAN MECHANICAL		INSIDE SPAN THERMAL		OUTSIDE SPAN MECHANICAL		OUTSIDE SPAN THERMAL		LOAD/PT	
	MPa	(PSI)	MPa	(PSI)	MPa	(PSI)	MPa	(PSI)	N	(LB)
	LIMIT LONGITUDINAL CORE SHEAR STRESS (AVERAGE)									
1	-.461	(-66.9)	0	0	.387	(56.1)	.553	(80.2)	4359	(980)
2	-.741	(-107.5)	0	0	.622	(90.2)	.553	(80.2)	7006	(1575)
	ULTIMATE LONGITUDINAL CORE SHEAR STRESS (SKIN CRITICAL)									
1	-2.97	(-431)	0	0	2.49	(361)	.546	(79.2)	28077	(6312)
2	-2.50	(-362)	0	0	2.09	(303)	.498	(72.2)	23584	(5302)

TYPICAL ULTIMATE CORE SHEAR STRESS (FAILURE) = 3.38 MPa (490 PSI)

Figure 13. Longitudinal Core Shear Stress (Hand Analysis) at Support X = 45.72 cm

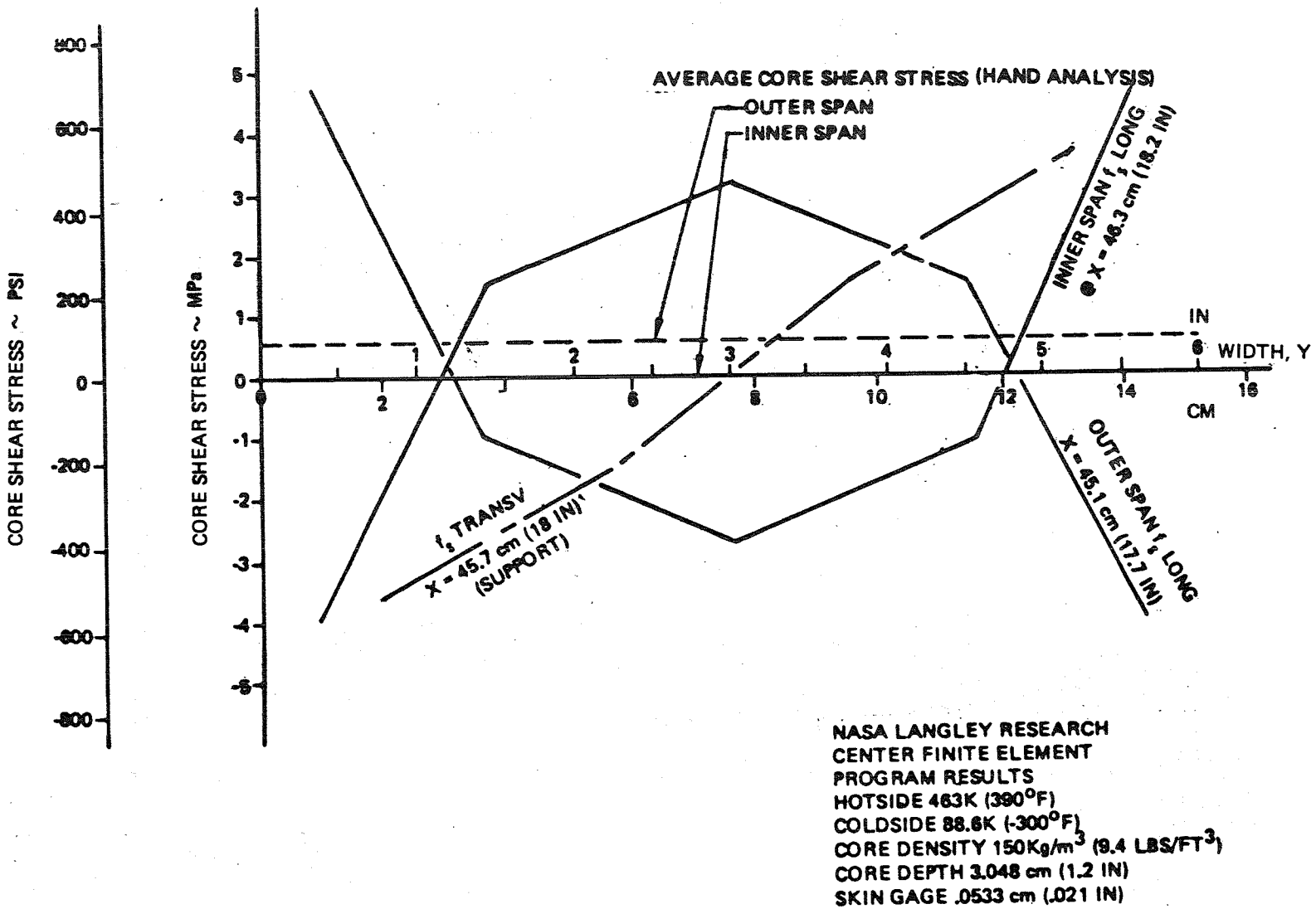

Figure 14. Specimen 2 Core Stresses Adjacent to or at X = 45.72 cm Support Due to Thermal Loads

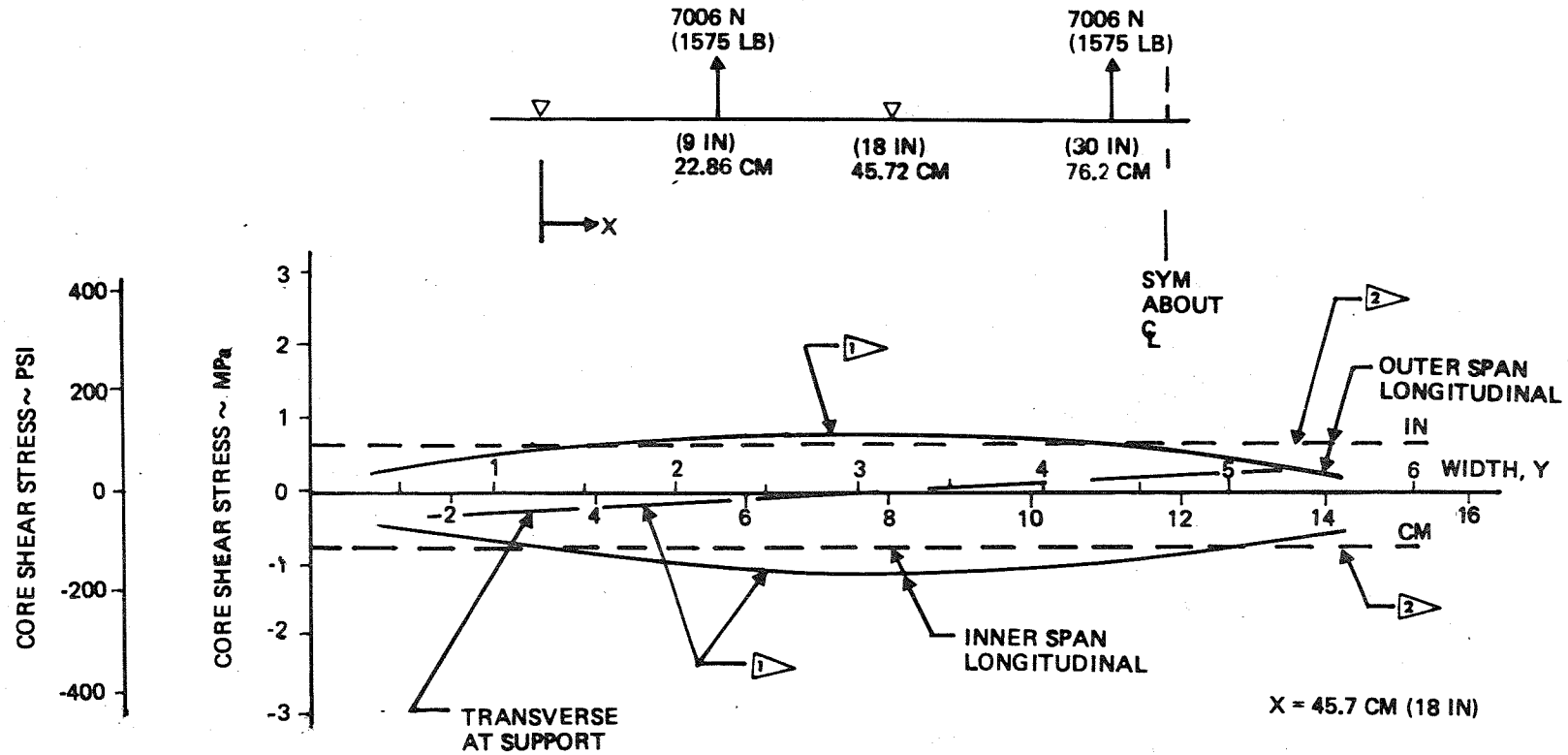

① NASA LANGLEY RESEARCH CENTER FINITE ELEMENT (SPAR) ANALYSIS USING 7006 N (1575 LB) AT FOUR LOAD POINTS

② HAND ANALYSIS

Figure 15. Specimen 2 Core Shear Stress at Interior Support Due to Mechanical Loads

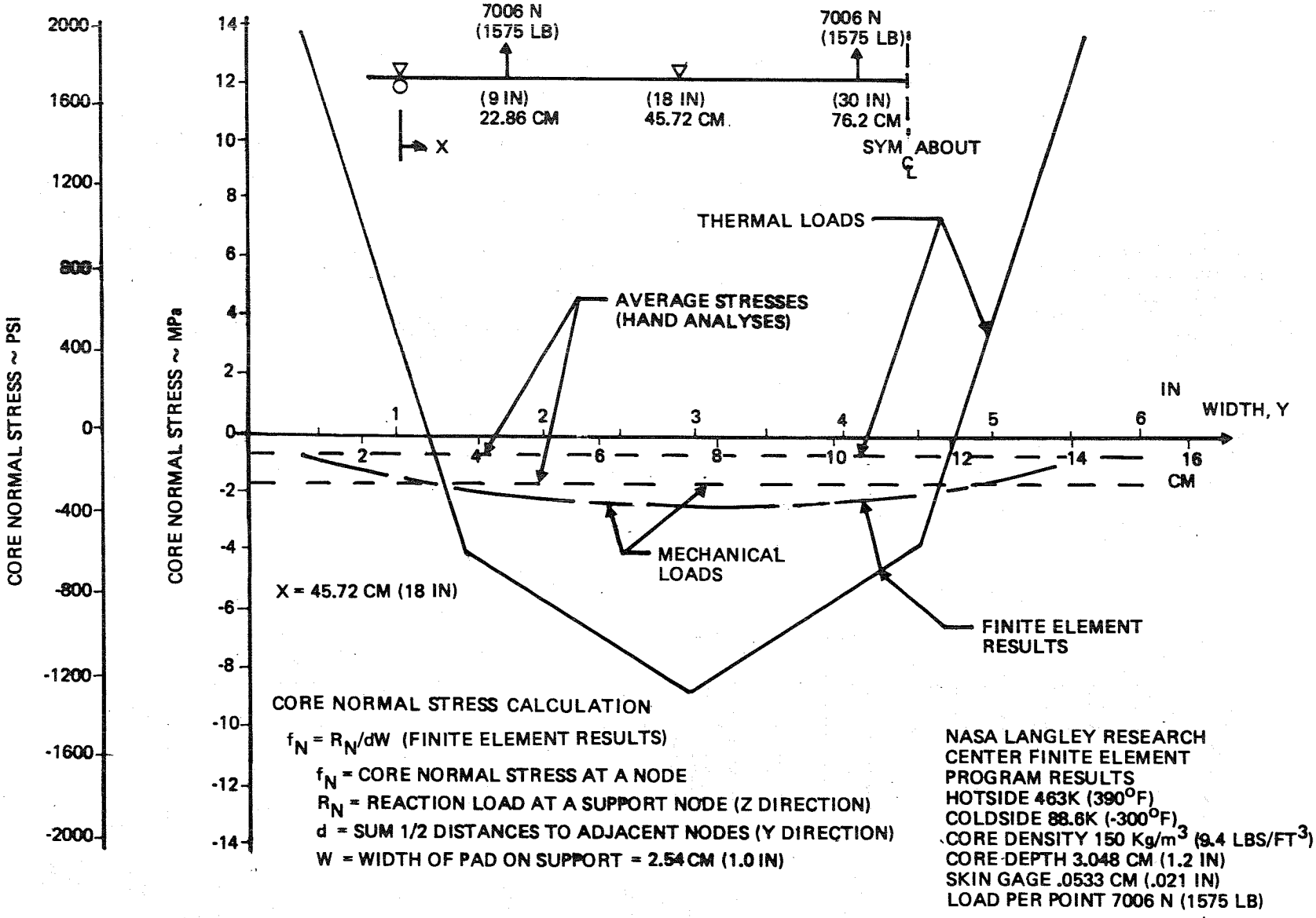

Figure 16. Specimen 2 Core Normal Stresses at Interior Support Due to Mechanical and Thermal Loads

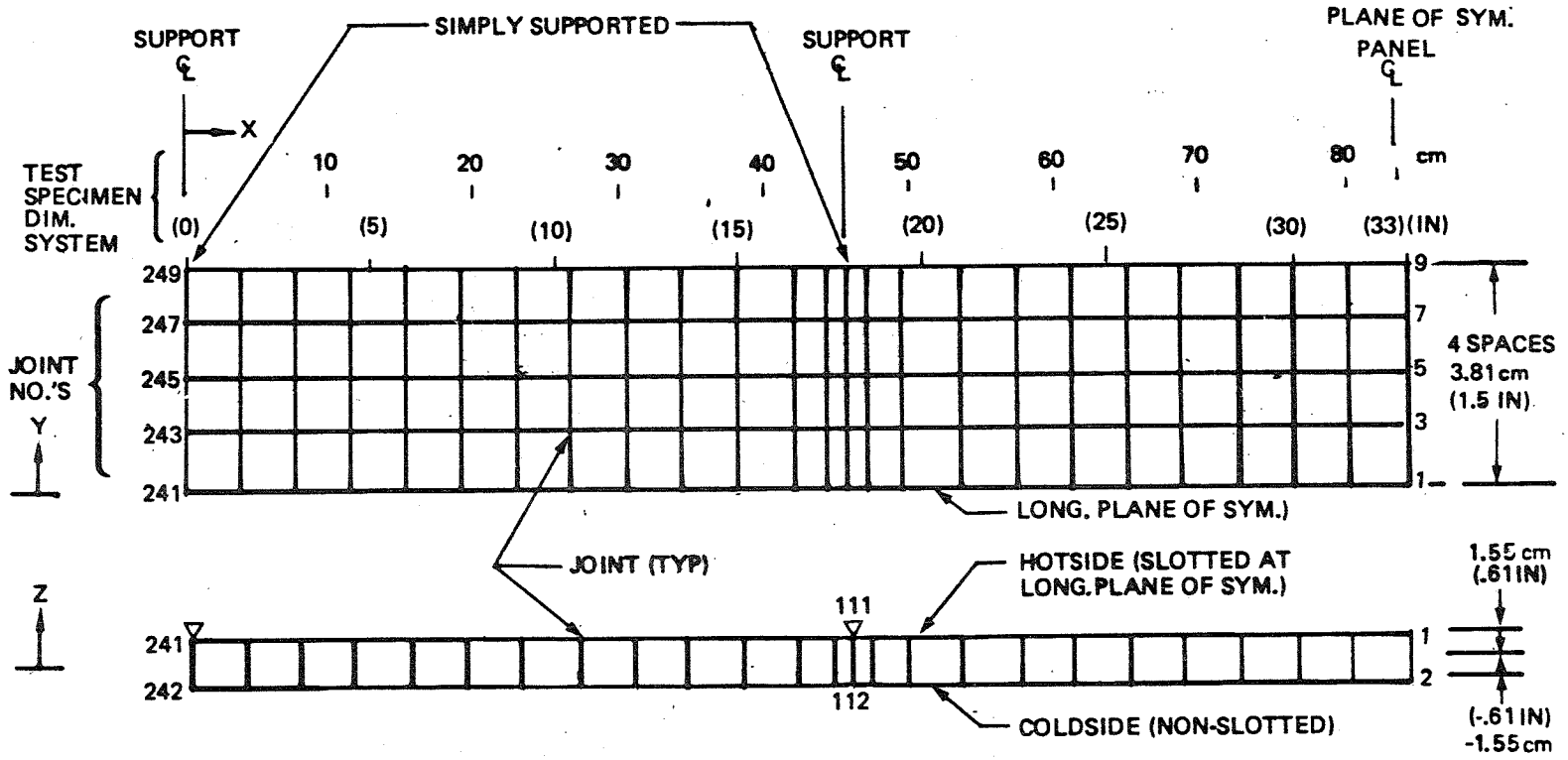

JOINT NO.	JOINT FIXITY δ_X	δ_Y	δ_Z	θ_X	θ_Y	θ_Z	
2	1	1	0	1	1	1	PANEL ℄ PLANE OF SYM.
1,3,4,5,6,7,8,9,10	1	0	0	1	1	1	
12 THRU 242 BY 10	0	1	0	1	1	1	COLD SURFACE ℄ INES, PLANE OF SYM
111,113,115,117,119	0	0	1	1	1	1	(INTERIOR SUPPORT NODES)
241,243,245,247,249	0	0	1	1	1	1	(END SUPPORT NODES)
OTHERS	0	0	0	1	1	1	

SPAR FINITE ELEMENT ANAL.
JAMES ROBINSON NASA LaRC
SKIN GA. .0533 cm (.021 IN)
CORE DEPTH 3.048 cm (1.2 IN)
CORE DENSITY 150 Kg/m^3
(9.4 LB/FT^3

Figure 17. Finite Element Model – NASA Langley Research Center

.076 CM (.03 IN.) GAGE RENE '41 SHEET SUBJECTED TO BRAZE AND AGE CYCLE							
ROOM TEMPERATURE TENSION STRESS (TYP.)				ELONGATION	NO. OF ENTRY CYCLES	ENTRY CYCLE MAX. TEMPERATURE	
ULTIMATE		YIELD					
MPa	KSI	MPa	KSI	%		K	°F
1289	187	869	126	24	–	–	–
1420	206	1020	148	14	500	1006	1350

Figure 18. Room Temperature Tensile Properties of Rene '41 Sheet Subjected to Braze and Age Cycle and Entry Cycle Thermal Exposures

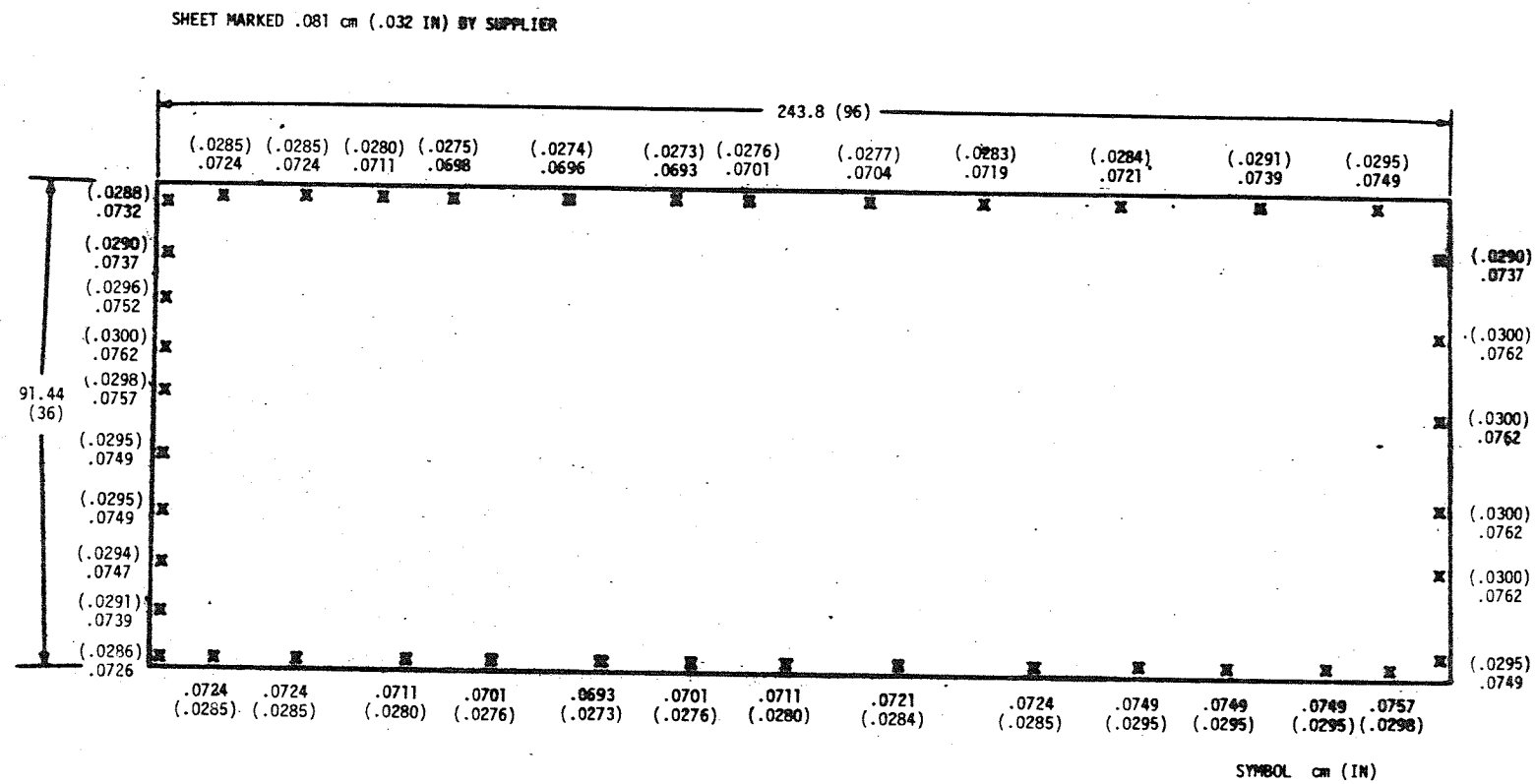

Figure 19. Specimen 1 Hotside Face Sheet Thickness Prior to Chem-Milling

LOCATION REF. FIGURE 2	DRAWING THICKNESS				CHEM MILLED THICKNESS	
	MIN	MAX	MIN	MAX		
	cm	cm	(IN)	(IN)	cm	(IN)
1	.051	.061	.020	.024	.058	.023
2	↓	↓	↓	↓	.058	.023
3	↓	↓	↓	↓	.058	.023
4	.064	0.69	.025	.027	.066	.026
5	↓	↓	↓	↓	.064	.025
6	↓	↓	↓	↓	.064	.025
7	.051	.061	0.20	.024	.058	.023
8	↓	↓	↓	↓	.058	.023
9	↓	↓	↓	↓	.058	.023
10	↓	↓	↓	↓	.058	.023
11	↓	↓	↓	↓	.057	.0225
12	↓	↓	↓	↓	.056	.022
13	↓	↓	↓	↓	.057	.0225
15	↓	↓	↓	↓	.055	.0215
14	↓	↓	↓	↓	.055	.0215
16	.064	.069	.025	.027	.064	.025
17	↓	↓	↓	↓	.064	.025
18	↓	↓	↓	↓	.064	.025
19	.051	.061	.025	.027	.058	.023
20	↓	↓	↓	↓	.056	.022
21	↓	↓	↓	↓	.056	.022

Figure 20. Specimen 1 Hotside Face Sheet Thickness After Chem-Milling

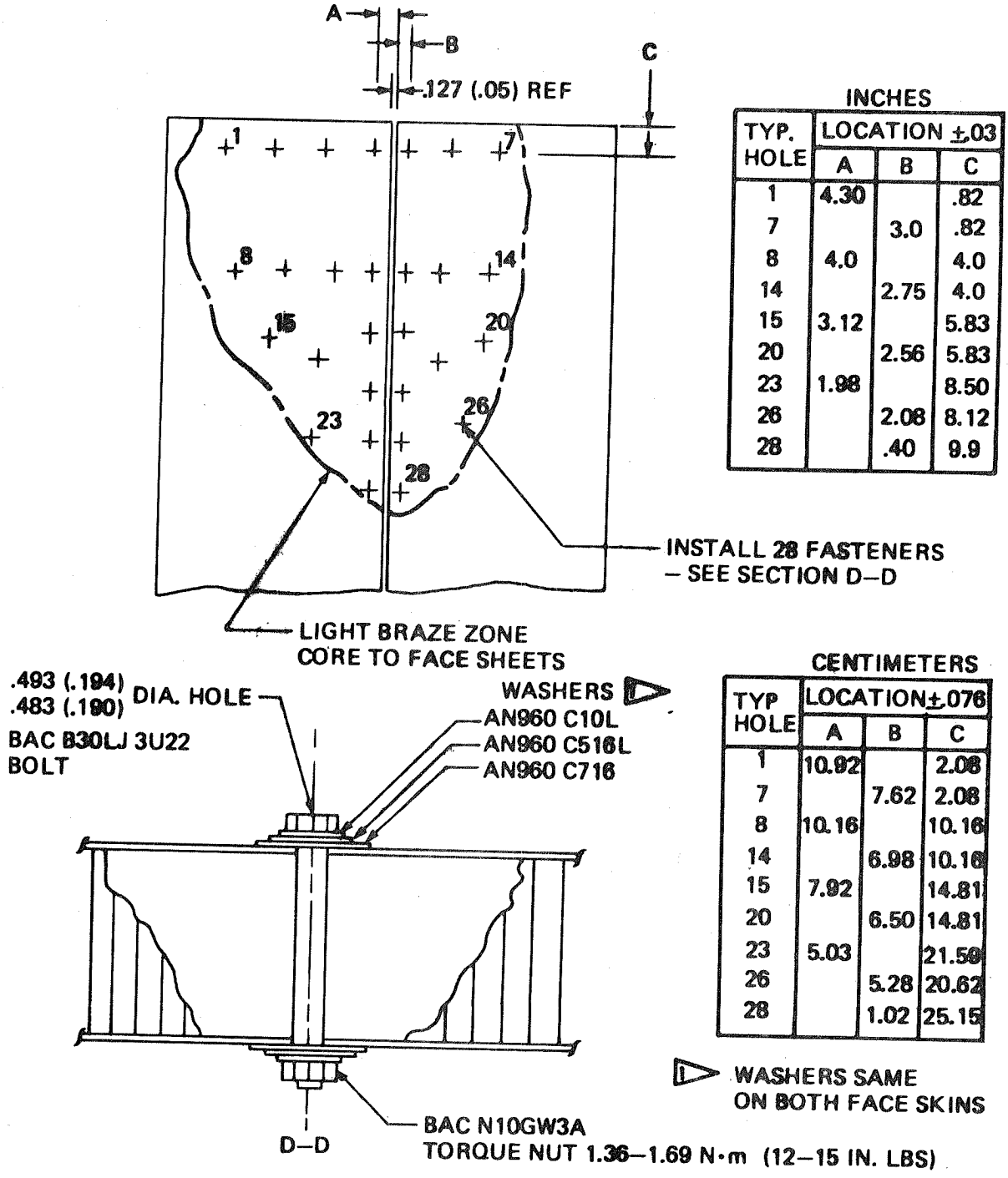

Figure 21. Specimen 1 Bolt Pattern in Light Braze Zone

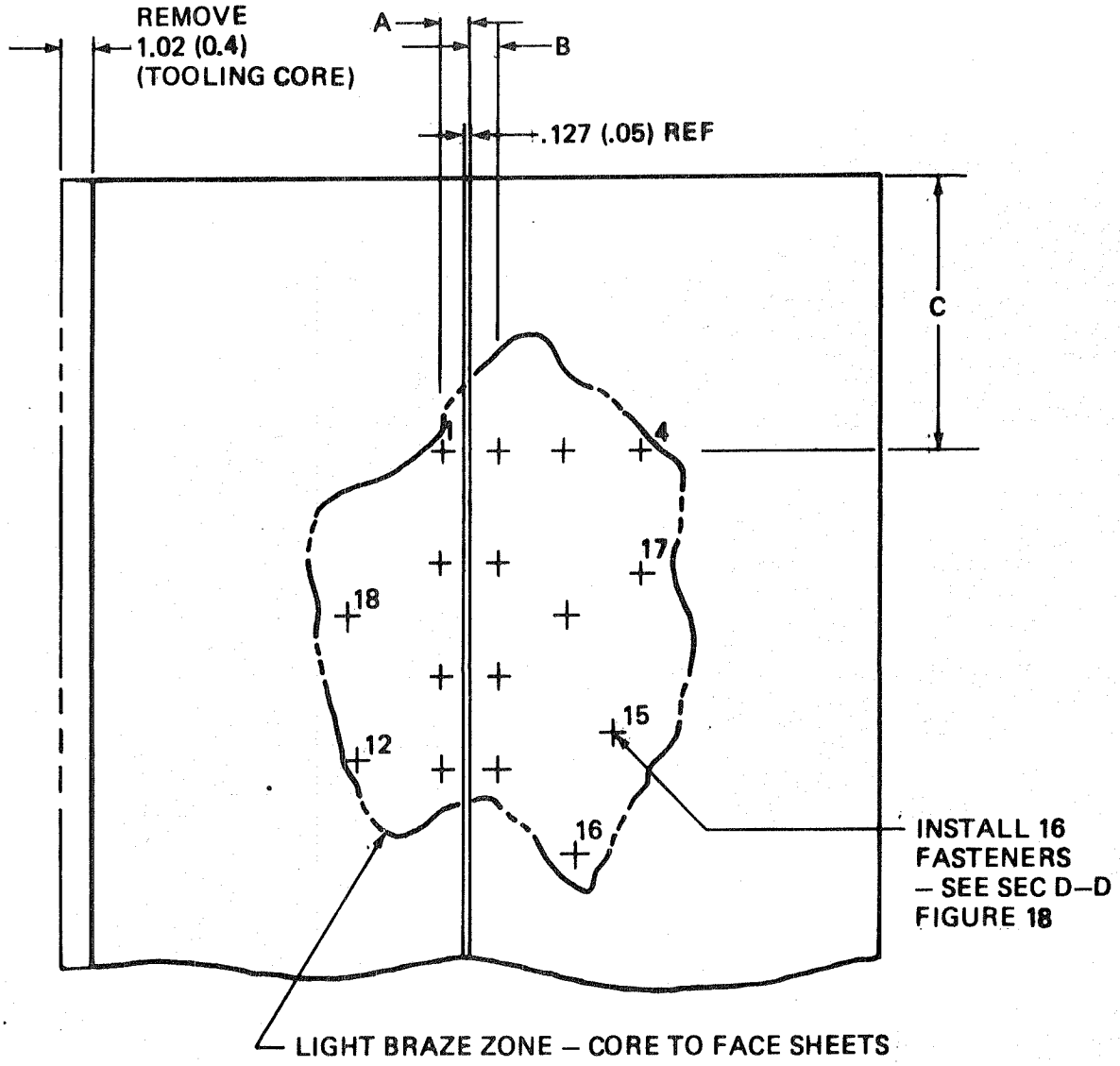

TYP. HOLE	CENTIMETERS LOCATION +.076			INCHES LOCATION +.03		
	A	B	C	A	B	C
1	1.02		10.03	.4		3.95
4		6.27	10.03		2.47	3.95
7		6.35	14.66		2.50	5.77
8	4.70		16.13	1.85		6.35
12	4.42		21.54	1.74		8.48
15	5.21		20.47		2.05	8.06
16	3.68		25.02		1.45	9.85

Figure 22. Specimen 2 Bolt Pattern in Light Braze Zone

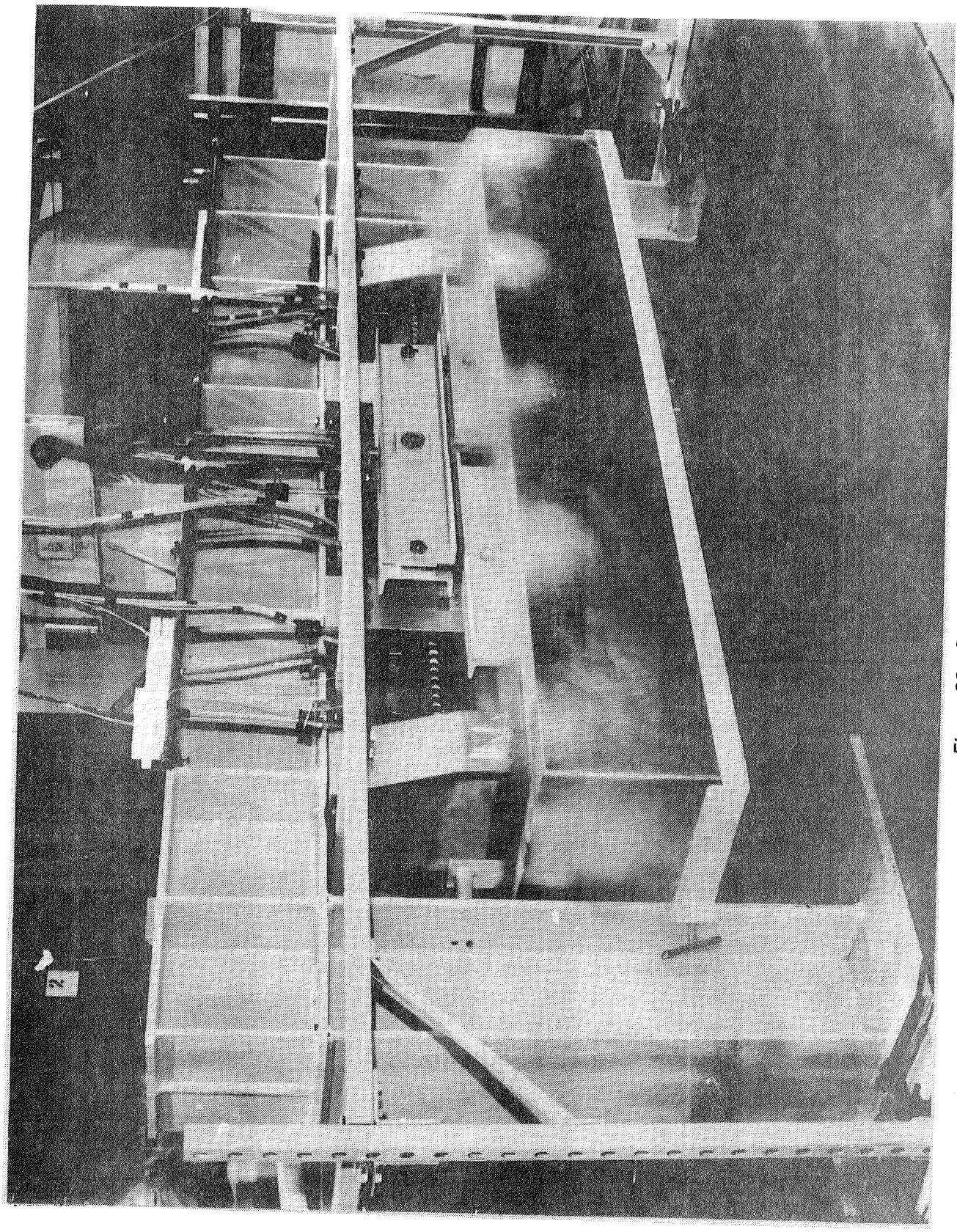

Figure 23. Panel Test Fixture

1. Report No.	2. Government Accession No.	3. Recipient's Catalog No.
NASA CR-165801		

4. Title and Subtitle	5. Report Date
DESIGN AND FABRICATION OF BRAZED RENÉ 41 HONEYCOMB SANDWICH STRUCTURAL PANELS FOR ADVANCED SPACE TRANSPORTATION SYSTEMS	December 1981
	6. Performing Organization Code

7. Author(s)	8. Performing Organization Report No.
Andrew K. Hepler and Allan R. Swegle	D180-26252-1
	10. Work Unit No.

9. Performing Organization Name and Address	11. Contract or Grant No.
Boeing Aerospace Company Kent, Washington 98031	NAS1-14213
	13. Type of Report and Period Covered
12. Sponsoring Agency Name and Address	Contractor Report
National Aeronautics and Space Administration Washington, D. C. 20546	14. Sponsoring Agency Code

15. Supplementary Notes

Langley Technical Monitor: John L. Shideler

Final Report - Task III

16. Abstract

The objective of this program was to design and fabricate two large brazed Rene'41 honeycomb panels and to establish a test plan and design and fabricate a test fixture to subject the panels to cyclic thermal gradients and mechanical loads equivalent to those imposed on an advanced space transportation vehicle during its boost and entry trajectories.

The panels will be supported at four points, creating three spans. The outer spans are 45.7 cm (18 in.) and the center span 76.2 cm (30 in.). Specimen width is 30.5 cm (12 in.).

The panels were primarily designed by boost conditions simulated by subjecting the panels to liquid nitrogen, 77K (-320°F) on one side and 455K (360°F) on the other side and by mechanically imposing loads representing vehicle fuel pressure loads. Entry conditions are simulated by radiant heating to 1034 K (1400°F).

The test program will subject the panels to 500 boost thermal conditions.

17. Key Words (Suggested by Author(s))	18. Distribution Statement
Brazed Honeycomb Sandwich Rene'41 Advanced Space Transportation Systems Thermal Stress Hot Structures	Unclassified - Unlimited Subject Category 39

19. Security Classif. (of this report)	20. Security Classif. (of this page)	21. No. of Pages	22. Price*
Unclassified	Unclassified	48	A03

For sale by the National Technical Information Service, Springfield, Virginia 22161

End of Document